HDAC3 controls male fertility through enzyme-independent transcriptional regulation at the meiotic exit of spermatogenesis

Summary:
6 supplementary figures
1 supplementary table

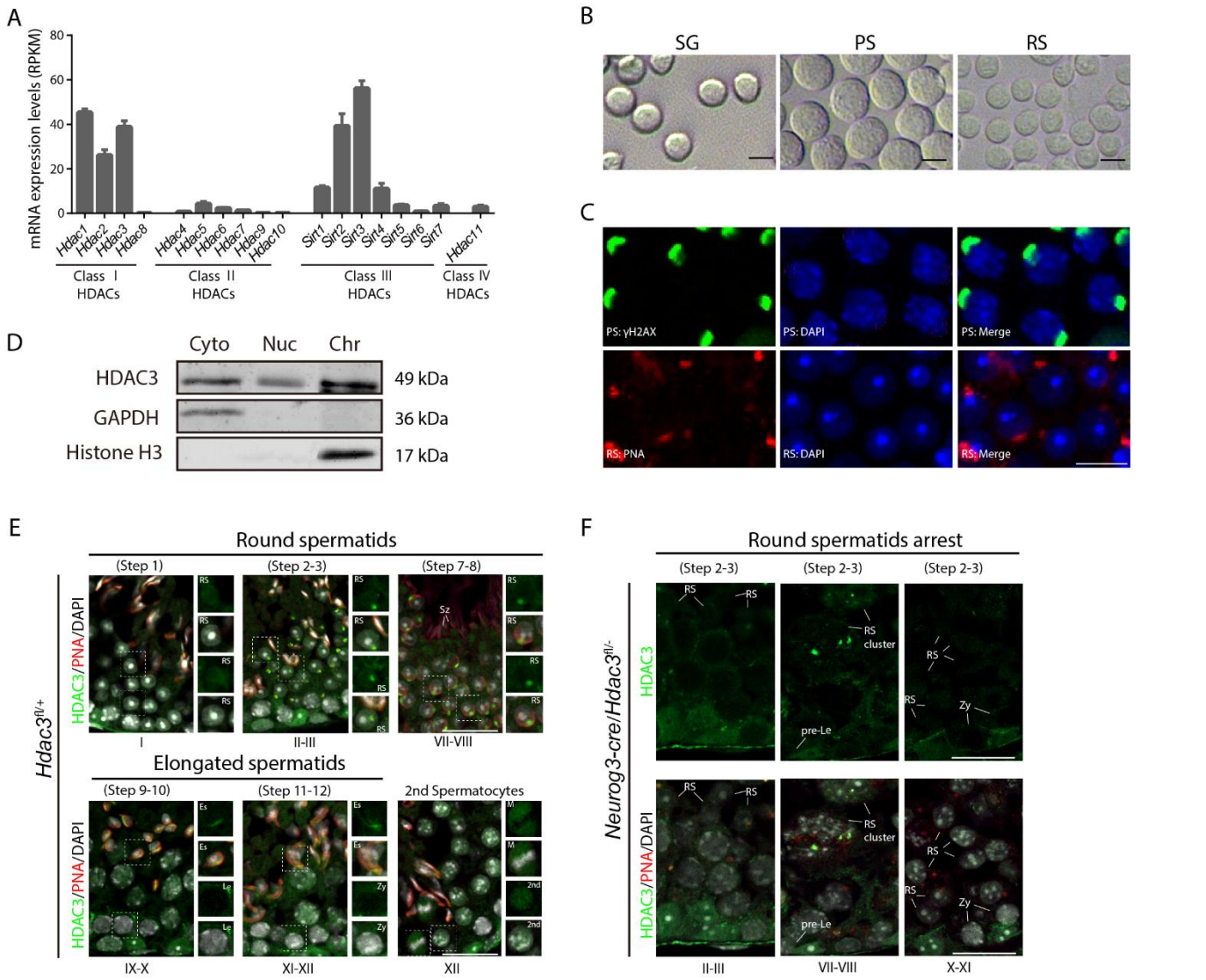

Figure S1. HDAC3 is selectively expressed in late spermatocytes and early RS at the late meiotic and early haploid stage. (**A**) mRNA transcripts levels of *Hdac* members in meiotic spermatocytes were assessed by RNA-seq. (**B**) Morphological analysis of purified germ cell populations. (**C**) Purities of isolated different types of mouse spermatogenic cells. Pachytene spermatocytes (PS), round spermatids (RS), and elongating spermatids (ES) were isolated from mice at age 7-8 weeks (n=8) and spermatogonia (SG) were isolated from mice at postnatal day 6-8 by STA-PUT method (n=20). Immunofluorescence staining of γH2AX and peanut agglutinin (PNA), which are specific protein markers for PS and RS, respectively. Scale bars, 20 μm. (**D**) Protein levels of HDAC3 in different factions of adult mouse testes (n=3). Protein samples were prepared from cytoplasmic extract, nuclear extract, and chromatin, and subjected to western analysis. GAPDH and Histone H3 are cytoplasmic and chromatin positive controls, respectively (**E-F**) Immunolabeling for HDAC3 (green), PNA (an acrosome marker, red), and Hoechst (DNA, gray) in postmeiotic germ cells on frozen sections from wild-type (**E**) and *Neurog3-cre*/*Hdac3*$^{fl/-}$ testes (**F**). The developmental steps of haploid spermatids were defined based on PNA staining. Scale bars, 25 μm.

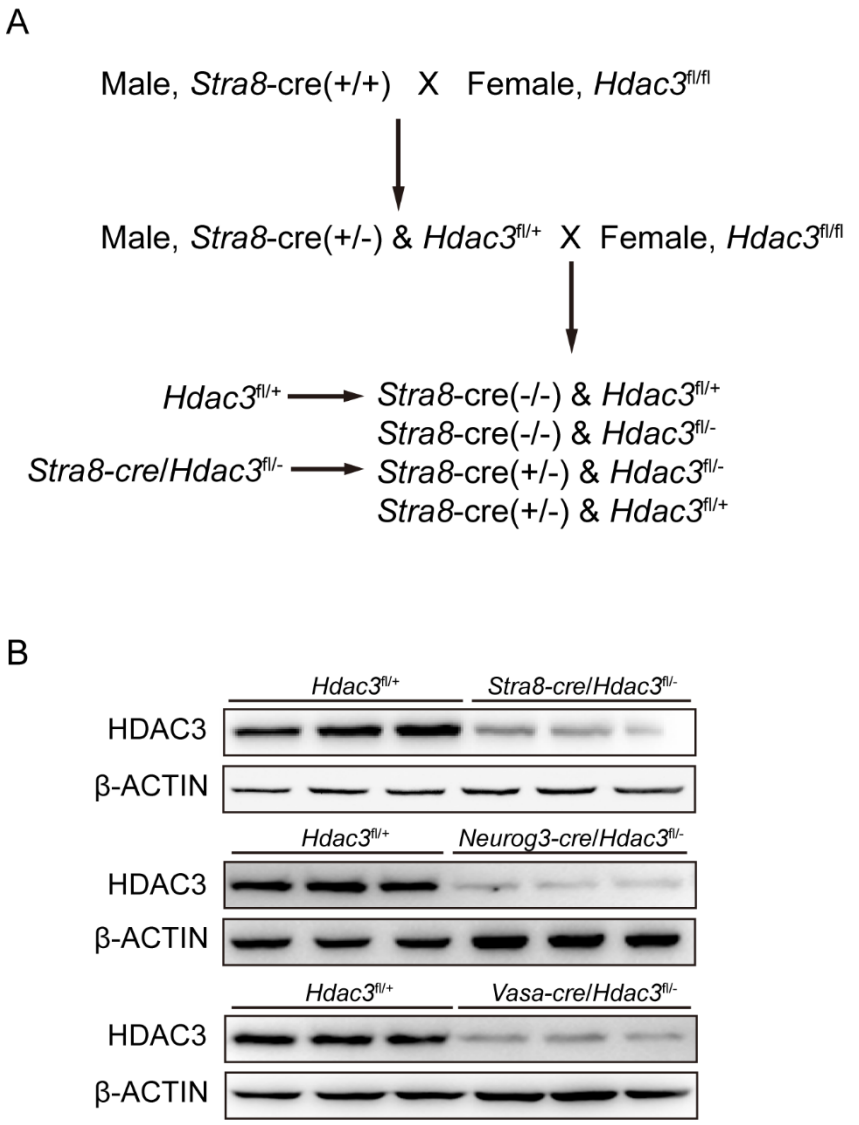

Figure S2. Three mouse lines with the testis-specific knockout of HDAC3 were established. (**A**) The breeding schemes for germ cell *Hdac3*-deficient mice. *Stra8-cre* is shown as one representative, and the same strategy was applied to generate *Vasa-cre* and *Neurog3-cre*/*Hdac3*$^{fl/-}$ mice. (**B**) Western blot showing the HDAC3 protein levels from wild type and *Vasa-cre*, *Neurog3-cre*, and *Stra8-cre*/*Hdac3*$^{fl/-}$ mice. Protein lysates were prepared from whole testis tissue at postnatal day 18. n=3 for each genotype. β-Actin was used as a loading control.

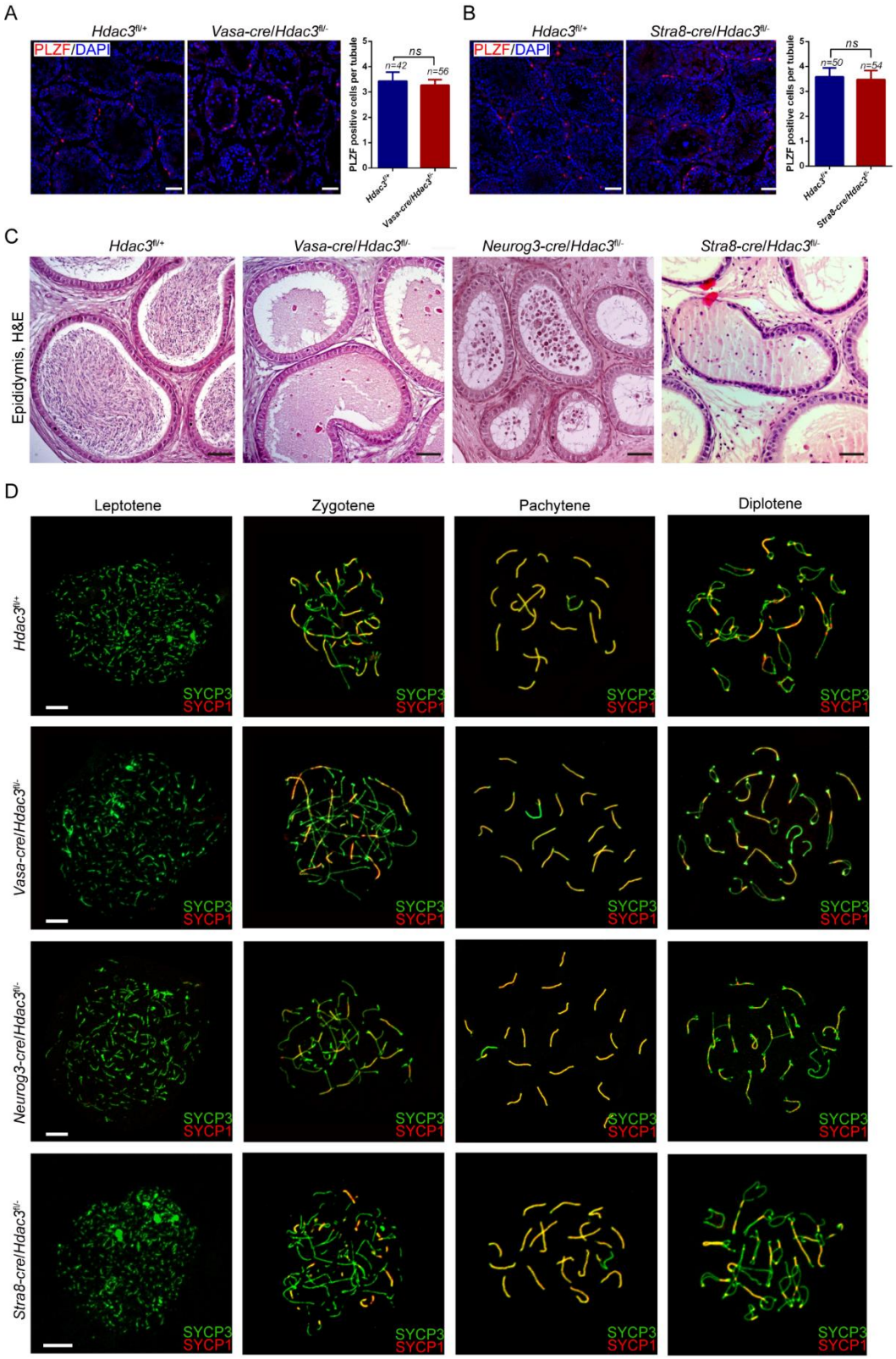

Figure S3. Normal spermatogonia and early meiotic prophase I in testis-specific HDAC3 knockout mice. (**A**) Frozen testes sections from adult *Hdac3*$^{fl/+}$ and *Vasa-cre*/*Hdac3*$^{fl/-}$ were immunostained for PLZF (red) and quantification of PLZF positive cells per tubule. (**B**) Immunofluorescence analysis with PLZF was performed on testes sections from adult *Hdac3*$^{fl/+}$ and *Stra8-cre*/*Hdac3*$^{fl/-}$ mice and quantification of PLZF positive cells per tubule. (**C**) Histologic analysis of epididymis from *Vasa-cre*, *Neurog3-cre*, and *Stra8-cre*/*Hdac3*$^{fl/-}$ mice and one representative *Hdac3*$^{fl/+}$ at 8-week-old. (**D**) Spread spermatocytes nuclei from 8-week-old *Hdac3*$^{fl/+}$, *Vasa-cre*, *Neurog3-cre*, and *Stra8-cre*/*Hdac3*$^{fl/-}$ mice were immunostained with antibodies against synaptonemal complex proteins SYCP3 (green) and SYCP1 (red). Scale bar, 10 μm.

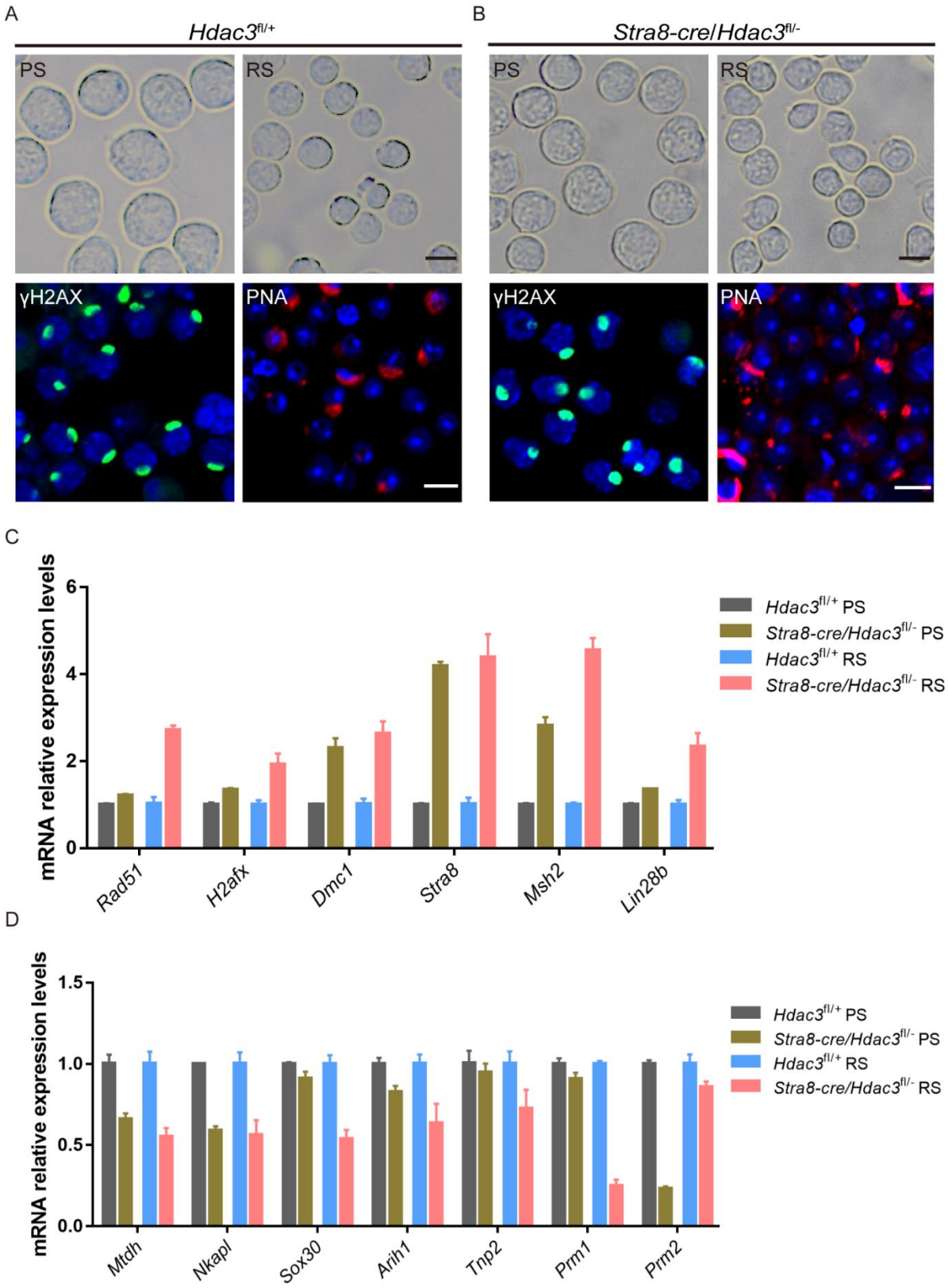

Figure S4. Expression of meiotic genes and postmeiotic haploid genes in *Stra8-cre*/*Hdac3*$^{fl/-}$ mice. (**A-B**) Morphological and immunofluorescence analysis of purified pachytene spermatocytes and round spermatids from adult *Hdac3*$^{fl/+}$ and *Stra8-cre*/*Hdac3*$^{fl/-}$ mice. γH2AX and PNA are protein markers for PS and RS, respectively. Scale bars, 20 μm. (**C-D**) RT-qPCR assays for exemplified genes either upregulated or downregulated in isolated PS and RS *Stra8-cre*/*Hdac3*$^{fl/-}$ mice. *Hdac3*$^{fl/+}$, n=6; *Stra8-cre*/*Hdac3*$^{fl/-}$, n=10 for each replicate. * $P < 0.01$, Student's t test.

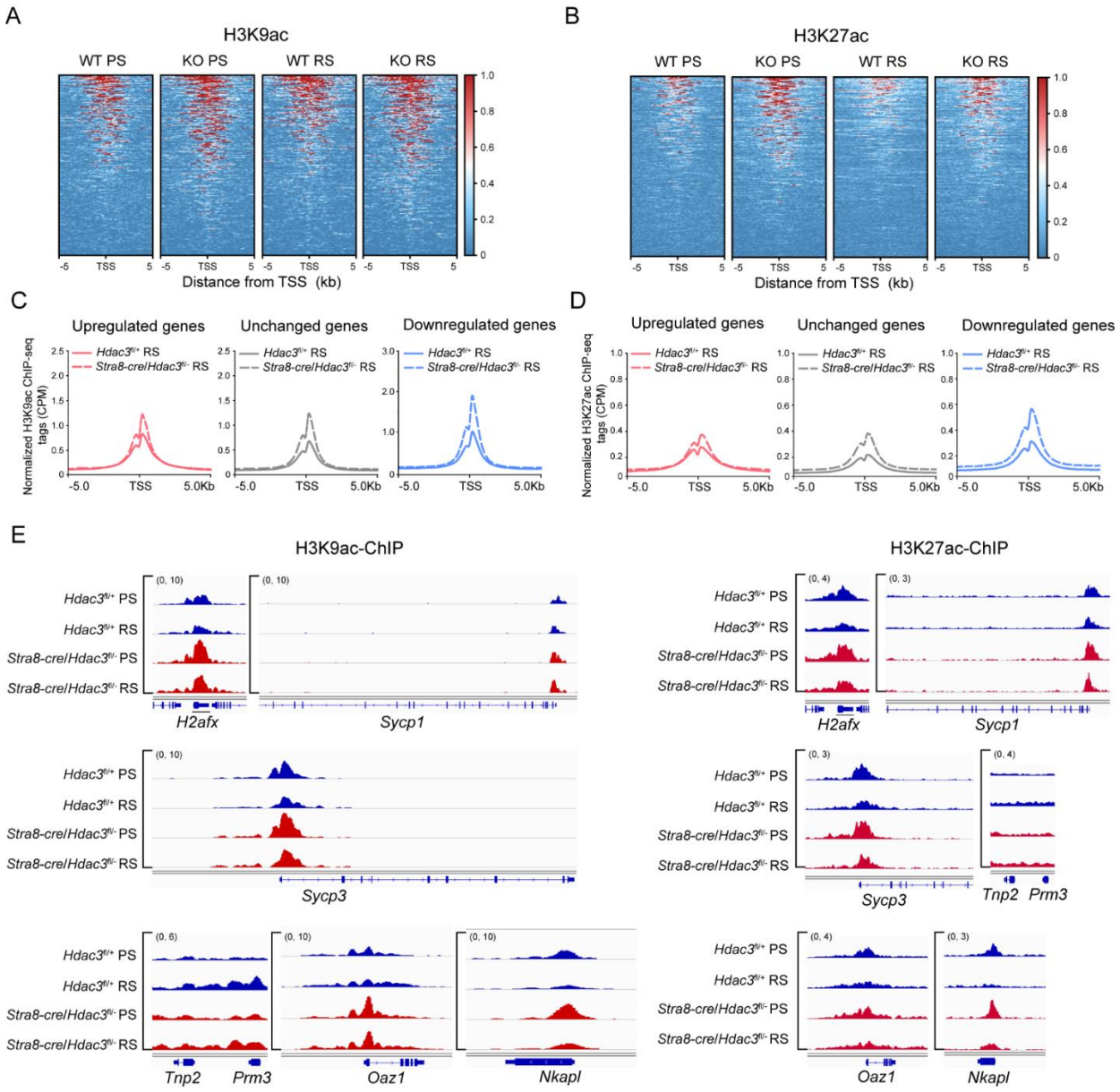

Figure S5. Histone acetylation near HDAC3 target genes in *Stra8-cre*/*Hdac3*$^{fl/-}$ mice. (**A-B**) Heat map of H3K9ac (**A**) or H3K27ac (**B**) ChIP-seq signals in PS and RS of the wild-type and *Stra8-cre*/*Hdac3*$^{fl/-}$ at HDAC3 binding sites near promoter regions. (**C-D**) Increased recruitment of H3K9ac (**C**) and H3K27ac (**D**) at upregulated (red), unchanged (gray) and downregulated (blue) genes in RS of *Stra8-cre*/*Hdac3*$^{fl/-}$ versus their wild-types. CPM, counts per million. (**E**) Genome browser tracks of representative loci highlighting H3K9ac and H3K27ac in WT and *Stra8-cre*/*Hdac3*$^{fl/-}$. *Y* axis scales represent reads per million.

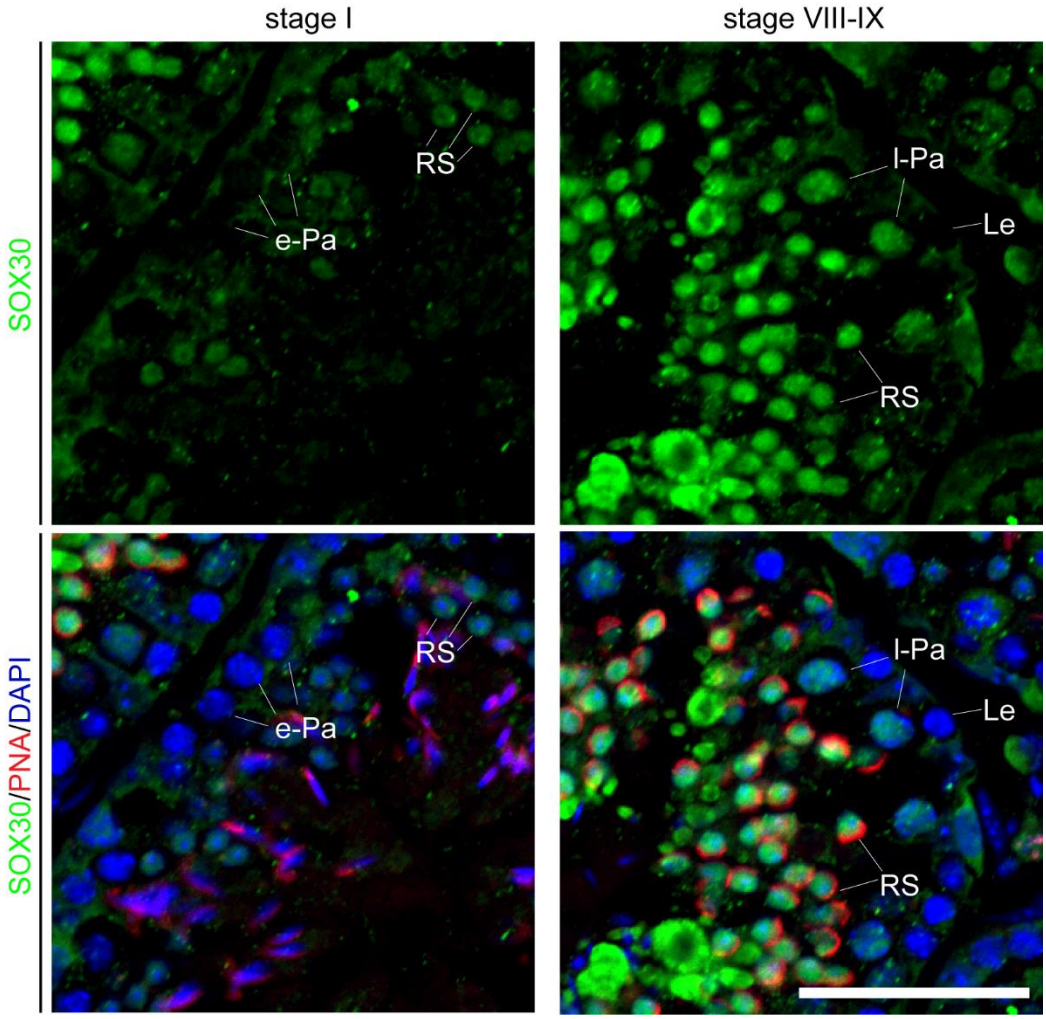

Figure S6. Distribution of SOX30 protein in mouse testis. Immunofluorecent staining was performed on adult testis sections with antibodies against SOX30 (green) and PNA (an acrosome marker, red). Seminiferous tubules at stage I and stage VIII-IX were shown. Le: leptotene; e-Pa: early pachytene; l-Pa: late pachytene; RS: round spermatids. Scale bars, 25 μm.

Supplementarty Table S1. Primers used in ChIP-qPCR and RT-qPCR

ChIP-qPCR	Forward	Reverse
Hexa	GCCTTGGGTTTGGGTTACAG	TCAGAGATCCGTAAGCAAAGG
Ilf3	GACCAAACCCGTGAGAGAAC	AGTAGGCGGGTGAGACGAA
Tnp2	CATGGACACCAAGATGCAGA	TGCACTGATTGCACTGGTTA
Sox30	GGGAACGTGCCTGTGATT	GATTGTGAGCTCAGCCGTTT
Mtdh	CACAGCCTCCACGTGACC	GGGACAGAGTGTCTCCAGAGG
Oaz1	CACTGCTTCGCCAGAGAGAA	GCTGTTTCTGGAAGGTTCGC
H2afx	GGCCGCCCAGCCCTCCCCACACC	GGCAAGCCGCCGCAGCCCGAAGT
Dmc1	CATCAAGGGGGCTTGCTC	ATTCTAACGCCGACCCAGA
Nkapl	GTCTGGAGAACGACCGCTAC	TTTCCTTCTCCTGGTCCTCA
RT-qPCR	Forward	Reverse
Msh2	GTGCAGCCTAAGGAGACGC	CTGGGTCTTGAACACCTCGC
Stra8	ACAACCTAAGGAAGGCAGTTTAC	GACCTCCTCTAAGCTGTTGGG
Rad51	AAGTTTTGGTCCACAGCCTATTT	CGGTGCATAAGCAACAGCC
Dmc1	ATGAAGGAGGATCAAGTTGTGC	CATGCTTCTGCAACAGGTCAA
Mtdh	TGCTCTTCCTTCTAGGTTACGG	CCATTTGGTTTGGGCTTTTCAG
H2afx	TACCTCACTGCCGAGATCCT	AGCTTGTTGAGCTCCTCGTC
Lin28b	TAGGTGGAGACGGCAGGATTT	ACCACAGTTGTAGCATCTTGGA
Nkapl	ATGTCGCCTGTATCCCGATCT	GTAGCGGTCGTTCTCCAGA
Sox30	ACCTGTCGGTGGGATCTCG	CAGCCTACAATCGTCCCTGG
Arih1	CAGGAGGAGGATTACCGCTAC	CTCCCGGATACATTCCACCA
Tnp2	GTGCACTCTCGACACTCACCT	AGCTACGCCTCTTAGCTCTGTG
Prm1	CCGTCGCAGACGAAGATGTC	CACCTTATGGTGTATGAGCGG
Prm2	TCCACAAGAGGCGTCGGTCAT	ACCTGCATCTCCTCCTCCTTCG
36B4	GCAGATCGGGTACCCAACTGTTG	CAGCAGCCGCAAATGCAGATG